Title

Effect of Ocrelizumab on B- and T-Cell Receptor Repertoire Diversity in Patients With Relapsing Multiple Sclerosis From the Randomized Phase III OPERA Trial

Journal

Neurology Neuroimmunology & Neuroinflammation, 10(4)

ISSN

2332-7812

Authors

Laurent, Sarah A
Strauli, Nicolas B
Eggers, Erica L
et al.

Publication Date

2023-07-01

DOI

10.1212/nxi.0000000000200118

Peer reviewed

RESEARCH ARTICLE OPEN ACCESS

Effect of Ocrelizumab on B- and T-Cell Receptor Repertoire Diversity in Patients With Relapsing Multiple Sclerosis From the Randomized Phase III OPERA Trial

Sarah A. Laurent, PhD,* Nicolas B. Strauli, PhD,* Erica L. Eggers, BA,* Hao Wu, MD, Brady Michel, PhD, Stanislas Demuth, MD, MSc, Arumugam Palanichamy, PhD, Michael R. Wilson, MD, Marina Sirota, PhD, Ryan D. Hernandez, PhD, Bruce Anthony Campbell Cree, MD, PhD, Ann E. Herman, PhD, and H.-Christian von Büdingen, MD

Correspondence
Dr. von Büdingen
h-christian.von_buedingen@roche.com

Neurol Neuroimmunol Neuroinflamm 2023;10:e200118. doi:10.1212/NXI.0000000000200118

Abstract

Background and Objectives

The B cell–depleting anti-CD20 antibody ocrelizumab (OCR) effectively reduces MS disease activity and slows disability progression. Given the role of B cells as antigen-presenting cells, the primary goal of this study was to evaluate the effect of OCR on the T-cell receptor repertoire diversity.

Methods

To examine whether OCR substantially alters the molecular diversity of the T-cell receptor repertoire, deep immune repertoire sequencing (RepSeq) of $CD4^+$ and $CD8^+$ T-cell receptor β-chain variable regions was performed on longitudinal blood samples. The IgM and IgG heavy chain variable region repertoire was also analyzed to characterize the residual B-cell repertoire under OCR treatment.

Results

Peripheral blood samples for RepSeq were obtained from 8 patients with relapsing MS enrolled in the OPERA I trial over a period of up to 39 months. Four patients each were treated with OCR or interferon β1-a during the double-blind period of OPERA I. All patients received OCR during the open-label extension. The diversity of the $CD4^+/CD8^+$ T-cell repertoires remained unaffected in OCR-treated patients. The expected OCR-associated B-cell depletion was mirrored by reduced B-cell receptor diversity in peripheral blood and a shift in immunoglobulin gene usage. Despite deep B-cell depletion, longitudinal persistence of clonally related B-cells was observed.

Discussion

Our data illustrate that the diversity of $CD4^+/CD8^+$ T-cell receptor repertoires remained unaltered in OCR-treated patients with relapsing MS. Persistence of a highly diverse T-cell repertoire suggests that aspects of adaptive immunity remain intact despite extended anti-CD20 therapy.

Trial Registration Information

This is a substudy (BE29353) of the OPERA I (WA21092; NCT01247324) trial. Date of registration, November 23, 2010; first patient enrollment, August 31, 2011.

*These authors contributed equally to this work.

From the Department of Neurology (S.A.L., E.L.E., H.W., B.M., S.D., A.P., M.R.W., B.A.C.C., H.-C.B.), Weill Institute for Neurosciences; Biomedical Sciences Graduate Program (N.B.S.); Bakar Computational Health Sciences Institute and Department of Pediatrics (M.S.); Department of Bioengineering and Therapeutic Sciences (R.D.H.), University of California, San Francisco, CA; Department of Human Genetics (R.D.H.), McGill University, Montreal, QC, Canada; and OMNI Biomarker Development (A.E.H.), Genentech, Inc., South San Francisco, CA.

Go to Neurology.org/NN for full disclosures. Funding information is provided at the end of the article.

The Article Processing Charge was funded by F. Hoffmann La-Roche.

Glossary

APC = antigen-presenting cell; **BCD** = B-cell depletion; **BCR** = B-cell receptor; **IGHV** = immunoglobulin heavy chain variable; **MG** = myasthenia gravis; **OCR** = ocrelizumab; **PCA** = principle components analysis; **PPMS** = primary progressive multiple sclerosis; **RMS** = relapsing forms of multiple sclerosis; **SFS** = site frequency spectra; **TCR** = T-cell receptor.

Ocrelizumab (OCR; Ocrevus, Genentech, Inc. CA) is a humanized, B cell–depleting, anti-CD20 monoclonal immunoglobulin (Ig) G1 antibody for treating relapsing forms of multiple sclerosis (RMS) and primary progressive multiple sclerosis (PPMS).[1,2] B cells are antigen-presenting cells (APCs) and produce antibodies, forming the cornerstone of adaptive immunity.[3-5] Therefore, understanding how B-cell depletion (BCD) affects the adaptive immune function is crucial.

The adaptive immune repertoire summates unique B-cell receptors (BCRs) or T-cell receptors (TCRs) per individual at any given time. A complex machinery generates vastly diverse B- and T-cell repertoires, including somatic recombination of variable (V; BCR/TCR), diversifying (D; BCR heavy chain, TCR β-chain), and joining (J; BCR/TCR) germline segments; insertion of N-nucleotides at the V–D and D–J junctions of BCR heavy chain variable regions (VH); and somatic hypermutation of BCR VH and light chain variable regions (V kappa or V lambda). These mechanisms produce fingerprint-like molecular features potentially useful for assessing immune repertoire diversity and identifying the clonally related B and T cells over time/in spatially separated compartments.[6-9]

To what extent OCR affects TCR diversity remains unknown. In light of an overall favorable safety profile of OCR in the context of deep peripheral B-cell depletion, this study tested the hypothesis that OCR does not affect TCR repertoire diversity using immune repertoire sequencing (RepSeq) of longitudinally collected blood samples from patients from a clinical trial evaluating OCR for the treatment of RMS.

Methods

Patients and Samples

Longitudinal blood samples were collected from 8 patients at 1 site (University of California San Francisco) in a substudy (BE29353) of the OPERA I trial (WA21092; NCT01247324; first patient enrolment, August 31, 2011), assessing the safety and efficacy of OCR vs 44 μg subcutaneous interferon beta 1a (IFNβ1-a) 3 times weekly for the treatment of RMS. We studied 4 patients who received OCR continuously through the 96-week double-blind period and open-label extension (OLE) phase and 4 who received IFNβ1-a during the double-blind period (96 weeks) and then switched to OCR for the OLE. Baseline samples served as untreated references. Peripheral blood mononuclear cells (PBMCs) were prepared by standard Ficoll density gradient centrifugation using standard procedures; 5×10^6 PBMCs were used for B-cell flow cytometry; 1×10^7 PBMCs were stored at −80°C in RNA extraction buffer (RLT, Qiagen) for later mRNA extraction and B-cell RepSeq. The remaining PBMCs were cryopreserved in liquid nitrogen for later sorting of $CD4^+$ and $CD8^+$ T cells.

Flow Cytometry Analysis and Sorting

For B-cell flow cytometry, 5×10^6 PBMCs were blocked with Fc receptor (FcR) Block (Miltenyi Biotec) and incubated in the dark on ice for 20 minutes with the following antibodies: IgD Brilliant Violet 421 (BioLegend 11-26c.2a), CD19 FITC (BioLegend HIB19), CD38 PE (eBioscience 90), and CD27 APC (eBioscience O323). B-cell subsets were gated out of $CD19^+$ and defined as naive (N) $CD19^+IgD^+CD27^-$; unswitched memory $CD19^+IgD^+CD27^+$; double-negative $CD19^+IgD\text{-}CD27^-$; switched memory $CD19^+IgD\text{-}CD27^+$ $CD38^-$; plasmablast (PB) $CD19^+IgD\text{-}CD27hiCD38hi$ $CD138^-$; and plasma cells $CD19^{+-}$ IgD-CD27hiCD38hi $CD138^+$.

For T-cell flow cytometry, 5×10^6 PBMCs were blocked with FcR Block (Miltenyi Biotec) and incubated in the dark on ice for 20 minutes with the following antibodies: CD20 FITC (BioLegend 2H7), CD19 PC5.5 (BioLegend HIB19), CD3 APC (BioLegend), CD4 PE (BioLegend), and CD8 A750 (BioLegend). T-cell subsets were $CD3^+CD19^-$ and sorted as $CD3^+CD4^+CD8^-$ or $CD3^+CD4^-CD8^+$ T cells into RLT buffer (Qiagen) with 1% beta-mercaptoethanol and stored at −80°C for eventual RNA isolation. B- and T-cell flow analysis and sorting was performed on separate PBMC samples.

Immune Repertoire Sequencing (RepSeq)

The TCR-Vβ repertoire diversity was analyzed in sorted $CD4^+$ and $CD8^+$ T-cells separately. The B-cell repertoire diversity of IgM-VH and IgG-VH was determined in unsorted PBMCs. Total RNA from sorted $CD4^+$ and $CD8^+$ T-cells or PBMCs was extracted (RNeasy Micro Kit, Qiagen) and reverse transcribed (iScript cDNA Synthesis Kit, Bio-Rad). TCR-Vβ cDNA was amplified by PCR (Advantage 2 PCR Kit, Clontech) using barcoded reverse primers annealing to the TCRβ constant region (TRBC1/2) and a pool of 35 forward primers annealing to different T-cell receptor beta variable regions[10] modified for Ion Torrent sequencing. IgM/G-VH cDNA was amplified with custom forward primers targeting immunoglobulin heavy chain variable (IGHV) region gene families 1–7 and reverse primers annealing IgG or IgM constant regions with Ion Xpress barcodes to uniquely tag each subset/isotype before library prep.[11] cDNA samples underwent 30–35 cycles of PCR. PCR-amplified product was purified with 1.5% agarose gel and SYBR Safe and extracted using the Qiagen MinElute Kit. Gel-purified DNA was quantified using the Agilent High Sensitivity DNA Kit and Bioanalyzer and then diluted to 13.5 pM, creating an

equimolar DNA library. The DNA library underwent emulsion PCR using the Ion OneTouch2 System (Life Technologies) to bind and clonally expand DNA fragments onto Ion Sphere beads (ISPs) for sequencing. Enriched ISPs were quality control checked using a Qubit Fluorometer and sequenced on the Ion PGM System (Life Technologies) using 318 v2 chips.

Statistics and Bioinformatics

Statistical analyses were performed using GraphPad Prism (see figure legends for details); p Values <0.05 denote statistical significance (eMethods, links.lww.com/NXI/A849).

Diversity Analysis

Diversity Calculation

Diversities of BCR and TCR repertoires were calculated using the Shannon[12] diversity index.

$$H = \sum_{i=1}^{i=S} -p_i \times ln\ p_i$$

where S is the total number of clusters of clonally related sequences (clone clusters, eMethods, links.lww.com/NXI/A849) in a sample, and p_i is the relative proportion of the i th clone cluster.

Diversity Regression

Linear regression was used to determine which study elements were significantly affecting patients' immune repertoire diversity. To find the most parsimonious model for our data, we started with a simple linear model and incrementally increased its complexity while checking for improvements in fit to the IgG data. During this process, we included models accounting for the longitudinal nature of the data, including mixed models and correlation matrices accounting for autocorrelation between adjacent time points (eMethods, links.lww.com/NXI/A849). The resulting linear model befitting the data while yielding the lowest Akaike information criterion was as follows:

$$H_{i,j} = \beta_0 + \beta_T t_{i,j} + \beta_{ocr}\delta_O(i,j) + \beta_{reb}\delta_R(i,j) + \beta_i + \beta_{iT} it_{i,j} + \varepsilon_{i,j.}$$

In this model, $H_{i,j}$ represents Shannon diversity for the j th time point of patient i; $t_{i,j}$ represents time since baseline (weeks) for patient i's sample j; $\delta_O(i,j)$ is an indicator function equaling 1 if sample i,j was treated with OCR, and 0 otherwise; $\delta_R(i,j)$ is an indicator function equaling 1 if sample i,j was treated with IFNβ1-a, and 0 otherwise; and it is an interaction variable between time and patient. The βs represent effect sizes for each explanatory variable listed above, β_0 gives the y-intercept, and ε represents the error, constrained by being normally distributed with a mean of 0. We then fit this model to the Shannon diversity data from each immune repertoire (IgG and IgM for BCRs; CD4 and CD8 for TCRs) using the lm function in R. We interrogated which of the covariates in the model significantly affected diversity levels in each data set. While we left age uncorrected—despite its well-known effect on immune repertoire diversity[13,14]—we did correct for patient-specific effects, thus capturing any effect of age on diversity.

Site Frequency Spectra

Shannon diversity is a statistic derived from a complex distribution of frequencies. To investigate diversity, we generated site frequency spectra (SFS) for each sample. SFS plots are commonly used in population genetics to characterize the population diversity, illustrating the distribution of frequency values of the unique elements in a population. Herein, a unique element is defined as a single clone cluster, with our SFS plots showing the distribution of frequencies across all the clone clusters in a sample. Therefore, each analyzed unique clone cluster was put into a frequency bin, with SFS giving the relative proportion of clone clusters in each bin. The width of the frequency bins for samples of TCR and BCR data was 1/18,875 and 1/2,354, respectively (thresholds set by finding the number of sequences in the BCR and TCR RepSeq samples with the fewest sequences and then taking the inverse of those values [i.e., finding the frequency of a singleton]).

Principle components analysis (PCA) of the SFS data was run by including each sample's SFS as a row in the input matrix. Thus, each point in the PCA plots represents a dimensional reduction of the SFS of a single patient/time point.

V Gene Usage Analysis

V Gene Prevalence

We calculated the V gene prevalence, which quantifies a given V gene's representation in a sample, using 2 approaches. The first approach summated the number of clone clusters that use a given V gene while including the number of clone cluster–specific reads. The second approach counted the number of unique clone clusters using a given V gene (disregarding the read count information for each clone cluster) (eMethods, links.lww.com/NXI/A849).

The alternative—estimating clone frequency using deep-sequencing data—can be unreliable.[15] All statistical tests involving V gene prevalence thus used both approaches.

V Gene Prevalence Regression

We used the same linear model previously used to analyze the treatment effect on Shannon diversity to test whether OCR significantly affected the prevalence of a given V gene, except we replaced the dependent variable (previously Shannon diversity) with the V gene prevalence of a given V gene:

$$P_{i,j}(v) = \beta_0 + \beta_T t_{i,j} + \beta_{ocr}\delta_O(i,j) + \beta_{reb}\delta_R(i,j) + \beta_i + \beta_{iT} it_{i,j} + \varepsilon_{i,j}$$

The equation's right-side variables come from the Shannon diversity regression. Presumably, if OCR consistently affects a given V gene's prevalence across independent patients, a significant treatment effect would arise through this linear model, (i.e., OCR effect size, β_{ocr}, being significantly greater,

Table 1 Baseline Demographics and Disease Characteristics and Treatment Response of Patients Included in the Immune Response Repertoire Analysis

	Pt ID	Sex	Age	Previous MS treatment	Time since onset (y)	Time since Dx (y)	BL EDSS score	Pre-BL relapses	Relapses during treatment	BL T1 Gd+ lesions
OCR	MS-1	M	45	N	1	0.2	1.25	1	0	2
	MS-2	M	49	N	0.6	0.6	2.75	1	0	0
	MS-3	M	37	N	0.4	0.2	1.5	1	0	1
	MS-5	M	39	Y	3.7	1	1.5	1	0	1
IFNβ1-a → OCR	MS-4	F	53	N	4.6	4.6	1.25	1	0	0
	MS-6	F	34	Y	0.8	0.7	2.5	1	0	0
	MS-7	F	52	Y	5	4.4	2.75	2	0	1
	MS-8	F	32	N	0.8	0.1	2	1	1	0

Abbreviations: Age = age at enrollment; BL = baseline; Dx = diagnosis; EDSS = Expanded Disability Status Scale; Gd = gadolinium; IFN = interferon; OCR = ocrelizumab; Pt = patient.
The sex distribution (OCR all male and IFNβ1-a → OCR all female) was a chance result of the randomized selection process. All other clinical or paraclinical parameters were not significantly different between groups.

or less than zero; *t* test). This test was performed independently on each V gene represented in the RepSeq data.

Simulating B-Cell Demography

We used Wright-Fisher simulations[16-18] to account for possible bottlenecks imposed by OCR on the V gene prevalence data and for a bottlenecked demography in our BCR RepSeq data. Similar to reference 19 we used each patients' baseline sample to start each simulation set, and then used a multinomial sampling approach to simulate the following time point, iterating this process until the end of the time course. Conceptually, this process resembles putting all clone clusters from 1 time point into a bag and then randomly pulling them out to populate the next time point. Importantly, by incorporating our estimates of each samples' number of B cells, we were able to account for the bottlenecks that OCR induced in the B-cell population in our simulations (eMethods, links.lww.com/NXI/A849).

Standard Protocol Approvals, Registrations, and Patient Consents

All investigations were approved by the institutional review board (UCSF Committee on Human Research), and all patients provided written informed consent. This substudy (BE29353) of the OPERA I (WA21092; NCT01247324) trial was conducted in accordance with the Declaration of Helsinki.

Data Availability

RepSeq data are in the NCBI BioProject database (ncbi.nlm.nih.gov/bioproject/) under accession number PRJNA579384. For up-to-date details on Roche Global Policy on the Sharing of Clinical Information and how to request access to related clinical study documents, see here: go.roche.com/data_sharing. The Study Protocol and Statistical Analysis Plan were published.[1]

Results

Table 1 shows the study demographics. The gender distribution was due to chance during randomization that did not block sex-based treatment assignment.

Immunophenotyping Reveals Expected Effects of OCR Treatment on the B-Cell Compartment

Flow cytometry was performed before treatment start (baseline), 12 weeks after treatment initiation, every 24 weeks thereafter until week 96, at the start of the OLE, and until week 46 of the OLE for most patients. Because of limited patient sample availability, pretreatment baseline T-cell flow cytometry analysis could not be performed for 2 patients. See eTable 1 (links.lww.com/NXI/A850) for an overview.

Expectedly, a near-complete depletion of $CD19^+$ B cells occurred following OCR ($p < 0.05$). IFNβ1-a treatment did not affect B- or T-cell populations (Figure 1). In 2/4 OCR-treated patients (MS-1 and MS-3), some $CD19^+$ B-cell repopulation occurred between week 60 and the OLE baseline. The repopulating B cells included mostly naive, switched-memory, double-negative B cells and plasmablasts, whereas 1 patient (MS-5) showed a small, transient increase of the B-cell population, including unswitched and switched memory B cells, and plasmablasts (Figure 1, eFigure 1A, links.lww.com/NXI/A847). The overall $CD3^+$ T-cell compartment population and the $CD4^+$ and $CD8^+$ T-cell subtypes stochastically fluctuated over time but remained largely unaffected by OCR treatment (Figure 1B, eFigure 1, B and C).

OCR Reduces B-Cell but Not T-Cell Diversity

We generated RepSeq data for 8 patients, across 66 (Ig-VH) and 46 time points (TCR-Vβ). This totaled to 24,018,925 Ig-VH (median 137,624; range 260 -881,581) and 42,881,718

Figure 1 Flow Cytometric Analysis of Peripheral Blood Lymphocytes

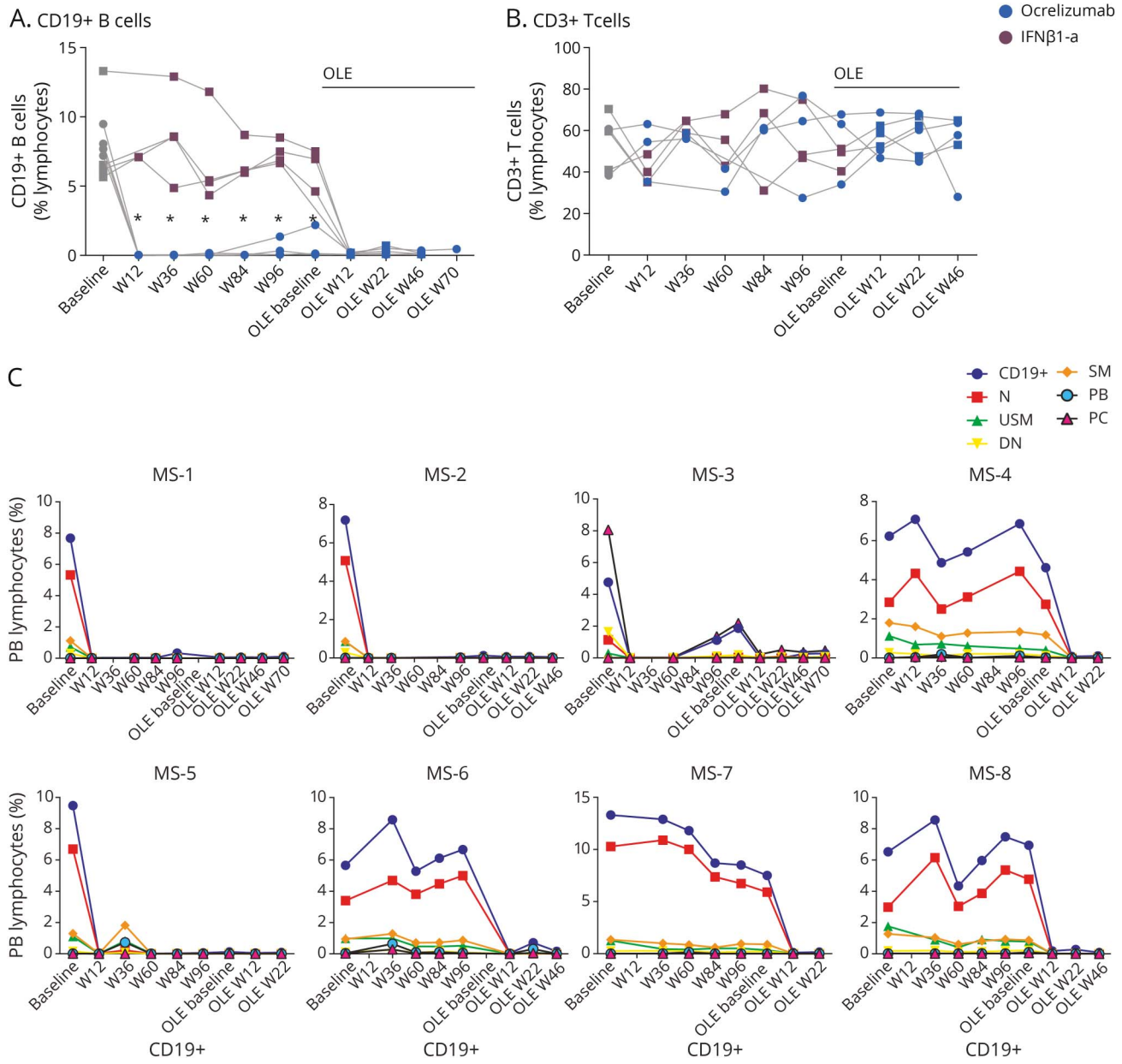

The percentage of $CD19^+$ B cells (A) and $CD3^+$ T cells (B) was determined in patients treated either with OCR (blue symbols) or with IFNβ1-a during the double-blind period (purple symbols). Peripheral B-cell subsets in patients treated with either OCR (MS-1, MS-2, MS-3, and MS-5) (C) or IFNβ1-a (MS-4, MS-6, MS-7, and MS-8) (D). B-cell subsets were gated out of $CD19^+$ and defined as naive (N) $CD19^+IgD^+CD27-$; unswitched memory (USM) $CD19^+IgD^+CD27^+$; double-negative (DN) $CD19^+IgD^-CD27^-$; (SM) $CD19^+IgD^-CD27^+$ $CD38^-$; plasmablast (PB) $CD19^+IgD^-CD27hiCD38hi$ $CD138^-$; and plasma cells (PCs) $CD19^+IgD^-CD27hiCD38hi$ $CD138^+$. *t test comparison, corrected for multiple tests using the Bonferroni-Dunn method, $p < 0.05$. IFN = interferon; OLE = open-label extension; W = week.

TCR-Vβ (median 445,352; range 148,973 -1,174,923), raw sequencing reads. After quality control and processing of raw sequencing reads (see Methods), 7,934,156 Ig-VH (median 37,250; range 16–389,852) and 17,614,523 TCR-Vβ (median 152,139; range 23,226–550,258) sequences were available for further analysis of clonal relatedness between time points and overall diversity in $CD19^+$ IgG/M-VH–expressing B cells and $CD4^+/CD8^+$ T cells contained within 1×10^7 peripheral blood mononuclear cells (PBMCs) (eTables 2–5, links.lww.com/NXI/A851, links.lww.com/NXI/A852, links.lww.com/NXI/A853, and links.lww.com/NXI/A854). RepSeq was performed at selected time points to reflect key events, including treatment initiation, treatment switch (IFNβ1-a to OCR), and longest available treatment interval, wherever possible based on sample availability (eTable 1, links.lww.com/NXI/A850).

To visualize the clonal diversity and relatedness between time points, circular networks were generated for IgM/G–Ig-VH and $CD4^+/8^-$TCR-Vβ (Figure 2, representative circle plots for 2 patients). To understand the clonal persistence over time, the percentage of clonal overlap between each time

Figure 2 Clonal Overlap and Relatedness

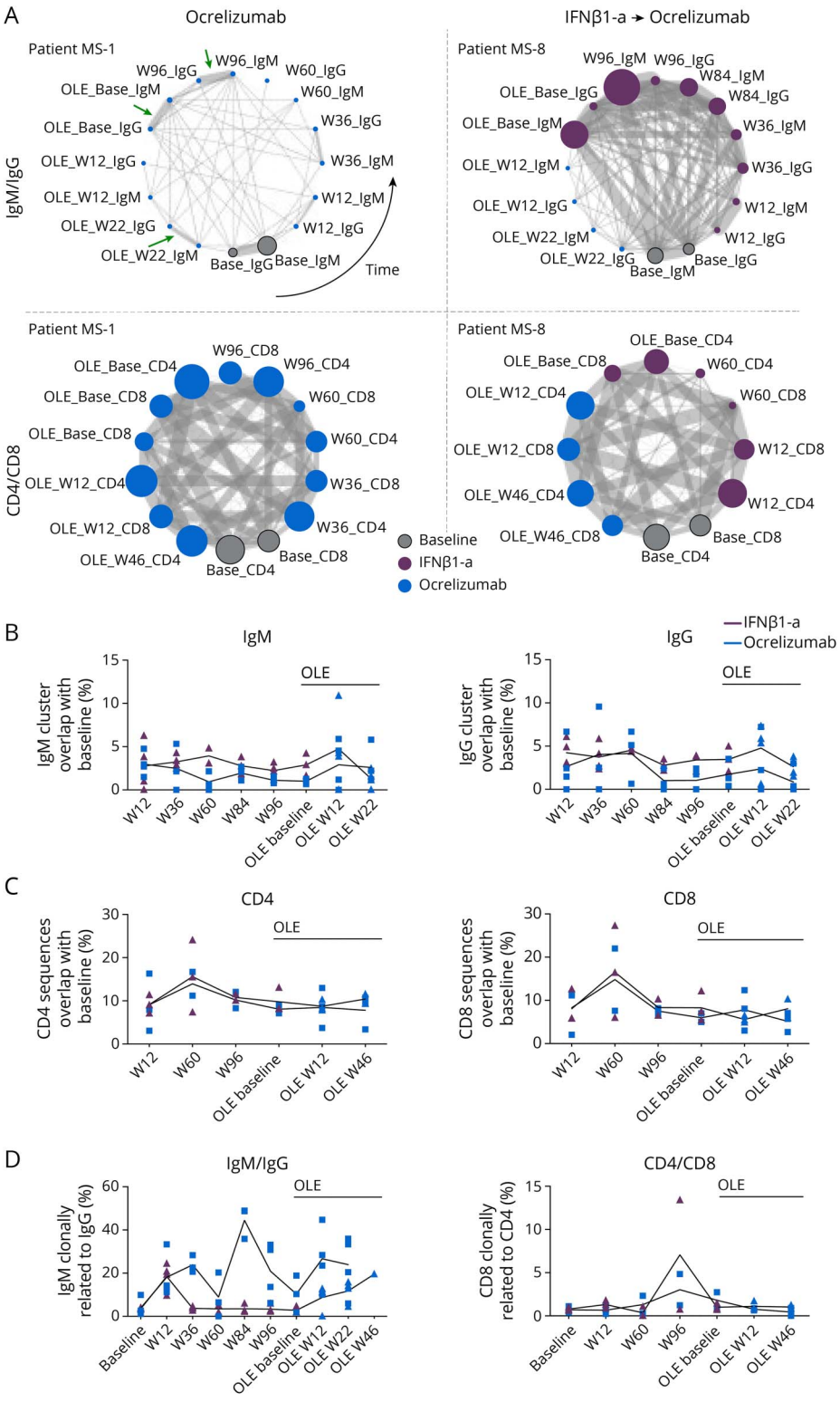

(A) Circular networks showing overall clonal diversity (node diameter) for IgM/G-Ig-VH and $CD4^+/8^-$TCR-Vβ contained within 1×10^7 PBMCs. Clonal relatedness (edges) between time points, Ig isotypes, or T-cell subsets were generated using Cytoscape. Longitudinal samples are plotted starting from baseline (gray nodes), with time progressing counterclockwise. Edges indicate related B cells or T cells in different samples (green arrows highlight relatedness between IgM-VH and IgG-VH). Node size and edge thickness are relative to number of Ig-VH clusters or connections, respectively. (B–D) Percent clonal overlap defined as the number of overlapping clone clusters between time point X and baseline, normalized by the total number of clone clusters at time point X, and then multiplied by 100. (B and C) The percentage of clonal overlap between each time point and baseline was calculated for the IgM-VH (B, left panel), IgG-VH (B, right panel), $CD4^+$TCR-Vβ (C, left panel), and $CD8^+$TCR-Vβ (C, right panel). (D) Percentage of IgM-VH repertoire clonally related to IgG-Ig-VH and the percentage of $CD8^+$TCR-Vβ repertoire clonally related to $CD4^+$TCR-Vβ. IFN = interferon; OLE = open-label extension; W = week.

Figure 3 Shannon Diversity Index for Ig-VH and TCR-Vβ Repertoire

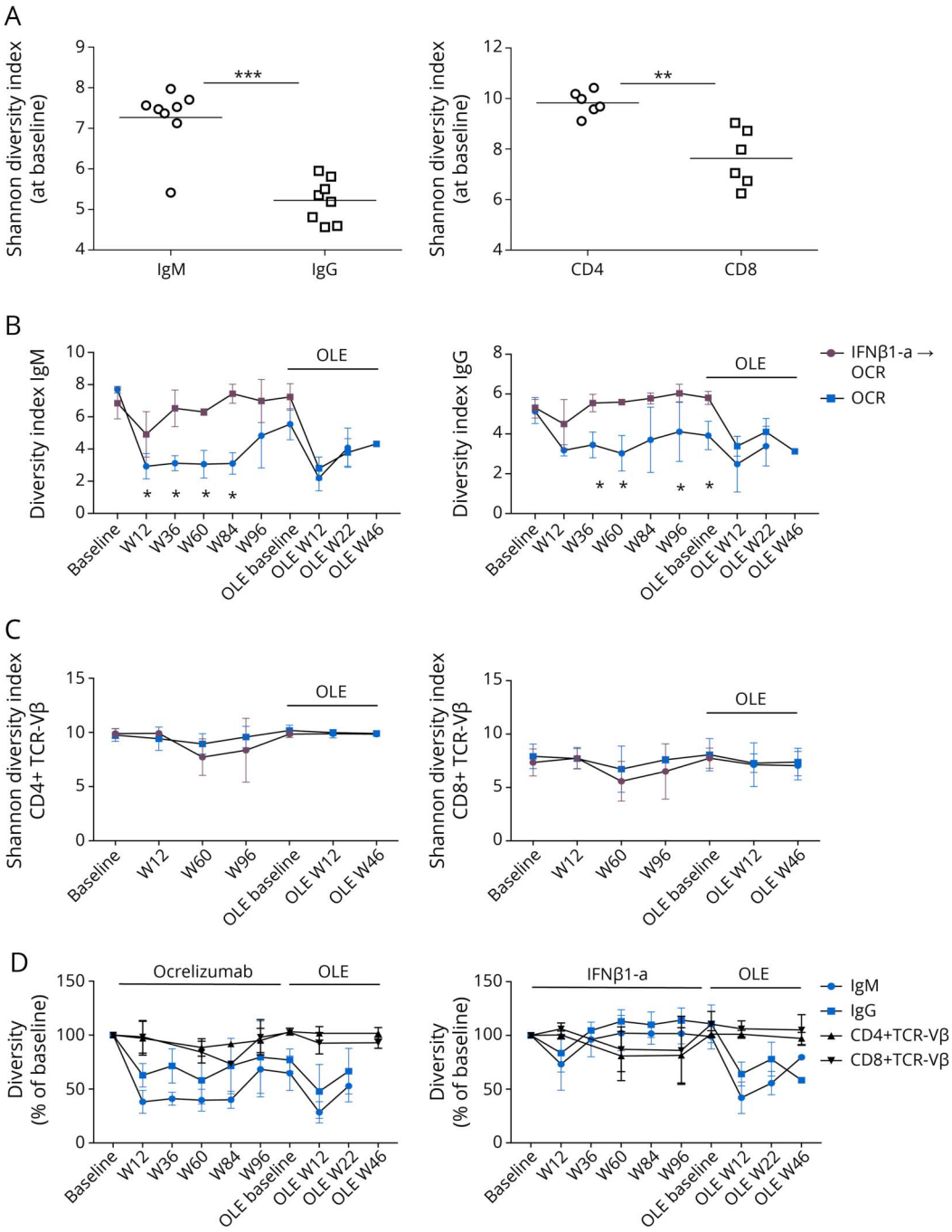

Diversity was calculated using the Shannon diversity index. Shannon diversity index at baseline for IgM-Ig-VH and IgG-Ig-VH, $CD4^+$TCR-Vβ, and $CD8^+$TCR-Vβ (A). Shannon diversity trajectories for Ig-VH (B) and TCR-Vβ (C) repertoire over time. (D) Shannon diversity was normalized to baseline (setting the baseline value to 100%), showing the effect of treatment OCR (left) and IFNβ1-a (right) on the diversity of IgM, IgG, $CD4^+$TCR-Vβ, and $CD8^+$TCR-Vβ repertoires. *t* test comparison, corrected for multiple tests using the Bonferroni-Dunn method, $*p < 0.05$, $**p < 0.01$, $***p < 0.001$, mean ± SD. Ig-VH = immunoglobulin–heavy chain variable region; OCR = ocrelizumab; OLE = open-label extension; TCR-V = T-cell receptor–variable region; W = week.

point and baseline was calculated for the following: IgM-VH (Figure 2B), IgG-VH (Figure 2B), $CD4^+$ TCR-Vβ (Figure 2C), and $CD8^+$ TCR-Vβ (Figure 2C). Despite extensive BCD, the fraction of clonal overlap of the Ig-repertoire between each time point and baseline was stable in OCR-treated patients (Figure 2B). Clonal relatedness between IgM-VH and IgG-VH at each time point was also found, potentially supporting ongoing class-switch recombination despite BCD (Figure 2D). Clonal persistence over time was also observed for the T-cell repertoire.

Diversity was calculated using the Shannon diversity index—a measure of a populations' richness and evenness. Expectedly, given the greater abundance and lower clonal expansion level

Table 2 Summary of Regression on Shannon Diversity Data

Variable	IgM (*p* Value)	IgG (*p* Value)	CD4 (*p* Value)	CD8 (*p* Value)
Time	0.97	0.12	0.67	0.96
IFNβI-a	0.02	0.76	0.24	0.62
OCR	3.29E-11	5.71E-07	0.77	0.81
Patient	0.06	0.05	0.78	0.1
Patient:Time	0.19	6.32E-04	0.82	0.77

Abbreviations: IFN = interferon; OCR = ocrelizumab.
Shows the significance of each covariate in our linear regression of diversity data in each of the immune repertoires. Patient:Time represents the interaction variable between time and patients.

of naive B cells in peripheral blood, IgM-VH showed greater baseline diversity than IgG-VH (Figure 3A). Greater diversity in TCR-Vβ from $CD4^+$ compared with $CD8^+$ T-cells was previously demonstrated in our study[20] (Figure 3A). In OCR-treated patients, a significant decrease of Shannon diversity index in the IgM and IgG repertoire of the remaining B cells was observed (Figure 3B), resembling that shown in previous reports for other anti-CD20 therapies.[6] The effect appeared stronger for the IgM repertoire (Figure 3B). In the OLE phase, treatment with OCR decreased IgM and IgG diversity in patients initially treated with IFNβ1-a, resembling levels observed in the patient group primarily treated with OCR (Figure 3B). Between week 84 and OLE baseline time points, a transient increase of the Ig-VH and IgM-VH Shannon diversity was observed, mirroring the low-level B-cell repletion seen in 2 patients (eFigure 1A, links.lww.com/NXI/A847).

We found no obvious relationship between minor infections (n = 4) or relapse (n = 1) with BCR diversity or B-cell subset composition (eFigure 1, D and E, links.lww.com/NXI/A847). However, we found a notable uptick in BCD diversity at weeks 96 and 100 in MS-2, MS-3, and MS-5—the time points most distanced from previous OCR infusion and thus most likely to exhibit B-cell repletion (eFigure 1D, third panel). These spikes were evident even at low flow cytometry B-cell levels (eFigure 1D, top panel), suggesting that RepSeq could help surveil B cells during BCD, potentially surpassing the sensitivity of flow-based assays. Last, we have not observed significant effect of OCR on the diversity of the TCR-Vβ repertoire of $CD3^+CD4^+$ and $CD3^+CD8^+$ T cells (Figure 3, C and D).

To statistically test which variables significantly affect the immune repertoire diversity, a multiple linear regression analysis was performed including Shannon diversity as the dependent variable and time, patient ID, treatment status, and an interaction between patient ID and time as the explanatory variables. This approach was applied to each available immune repertoire (IgG and IgM for BCRs; CD4 and CD8 for TCRs; eFigure 2, links.lww.com/NXI/A848). OCR (treatment status) significantly negatively affected Shannon diversity in the IgG and IgM data, unlike in the CD4 or CD8 data. In addition, IFNβ1-a did not affect diversity in any included data set. Table 2 summarizes the covariates significantly affecting diversity levels in these data sets ($CD4^+/8^+$TCR-Vβ and IgM/G-Ig-VH immune repertoires).

To explore the underlying structure of these immune cell populations, SFS plots were generated for each sample. SFS plots can help illustrate the frequency values distribution in a population. Herein, the SFS plots show the distribution of frequencies across all the unique clone clusters in a sample. We observed that the BCR samples (IgG and IgM) under OCR treatment exhibited a higher concentration of high-frequency clone clusters and lower concentration of lower-frequency clone clusters relative to the untreated (baseline) samples (Figure 4A). Contrastingly, BCR samples treated with IFNβ1-a had no appreciable difference in their SFS compared with the untreated samples (Figure 4A). The SFS of the TCR samples showed no obvious differences with respect to treatment or $CD4^+/CD8^+$ cell type (Figure 4B).

Principal component analysis (PCA) was performed to better visualize the general trends in the SFS plots. The SFS of all samples served as the input, where each row in the input matrix was the SFS of a single sample. In the BCR data, the first principal component (PC1) separated the OCR-treated samples from the untreated or IFNβ1-a–treated samples (Figure 4C). Contrastingly, OCR-treated and untreated samples remained unsegregated in the TCR data, with the observed larger range of TCR SFS in IFNβ1-a–treated participants implicating the treatment's effect on the T-cell repertoire (Figure 4C).

Unbalanced Effects of OCR on IGHV Usage

In the context of another autoimmune disease, myasthenia gravis (MG), incomplete BCD has been linked to disease relapse.[21,22] We thus sought to characterize the B-cell clones that persist post-OCR infusion by asking whether certain subsets of the B-cell populations are preferentially depleted relative to others and whether the prevalence of some V genes in the BCR RepSeq data is consistently affected due to OCR across independent patients. A multiple linear regression framework was used to model a given V gene's prevalence as

Figure 4 Site Frequency Spectra and Principal Component Analysis

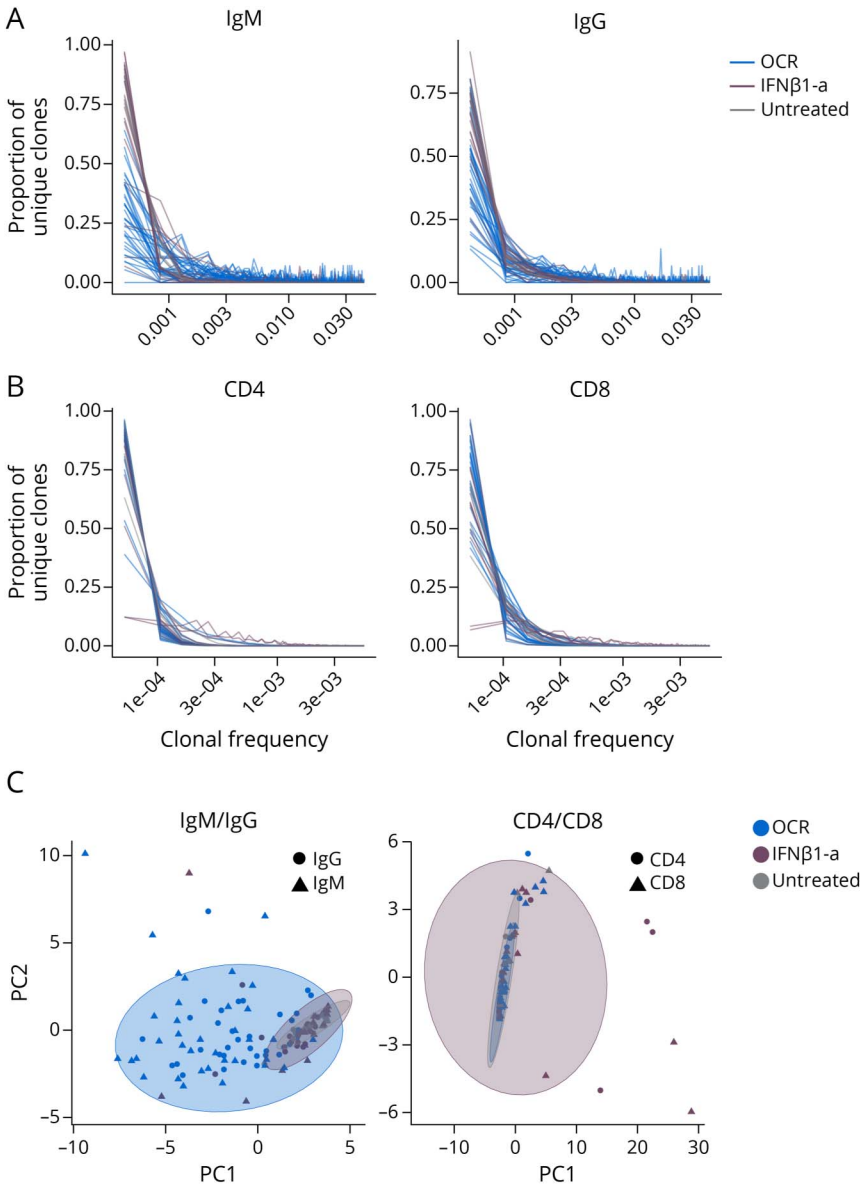

(A and B) Site frequency spectra showing the distribution of clone cluster frequencies for each sample. Each line corresponds to 1 sample, and color depicts treatment regimen. (A) Ig. (B) TCR-Vβ. (C) Principal component analysis of site frequency spectra data depicts the first (x-axis) and second (y-axis) principal components for Ig (left) and TCR-Vβ (right) repertoires. PC1 explained 20.0% and 71.2% of variance in Ig and TCR-Vβ data, respectively. PC2 explained 8.9% and 9.2% of variance in Ig and TCR-Vβ data, respectively. OCR = ocrelizumab; PC1 = principal component 1; PC2 = principal component 2; TCR-V = T-cell receptor–variable region.

the dependent variable across independent patients. This model was fitted to each V gene in the BCR data sets. Using this test, OCR had a significant effect on the prevalence of numerous V genes (Figure 5A). However, this test is confounded by OCR, which reduces the B-cell population. Because B cells are less numerous in OCR-treated samples, fewer V genes would conceivably be found. This scenario is analogous to the aforementioned bottlenecked demography. Wright-Fisher simulations[16-18] were applied to control the presumed effects on V-gene prevalence in the Ig RepSeq data. A regression-based test was performed on the simulated data, and the results were compared with the observed data (Figure 5A). OCR significantly affected V genes *IGHV1-69*, *IGHV6-1*, and *IGHV3-23* ($p < 0.05$, Benjamini-Hochberg corrected), showing a large effect size relative to the simulated data.

We then used this simulation framework to address (1) the unknown B-cell generation time (i.e., turnover rate, Figure 5B) and (2) the possibility of unreliable clone cluster frequency estimation from deep sequencing data (Figure 5, C and D). B-cell generation time was incorporated by simulating over a large array of possible values, and unreliable clone cluster frequency estimates were addressed by reducing their frequency values to presence or absence (i.e., 1 or 0, eMethods, links.lww.com/NXI/A849). The latter step was taken to account for potential PCR amplification biases, where true clone cluster frequency may not be preserved with high fidelity post-PCR amplification—a known issue for RepSeq.[15] We thus removed the clone cluster frequency information and summated the number of unique clone clusters using a given V gene. The gene-by-gene tests described above were repeated, and the V

Figure 5 Comparing the Effect of Ocrelizumab on Observed to Simulated Gene Prevalence Data

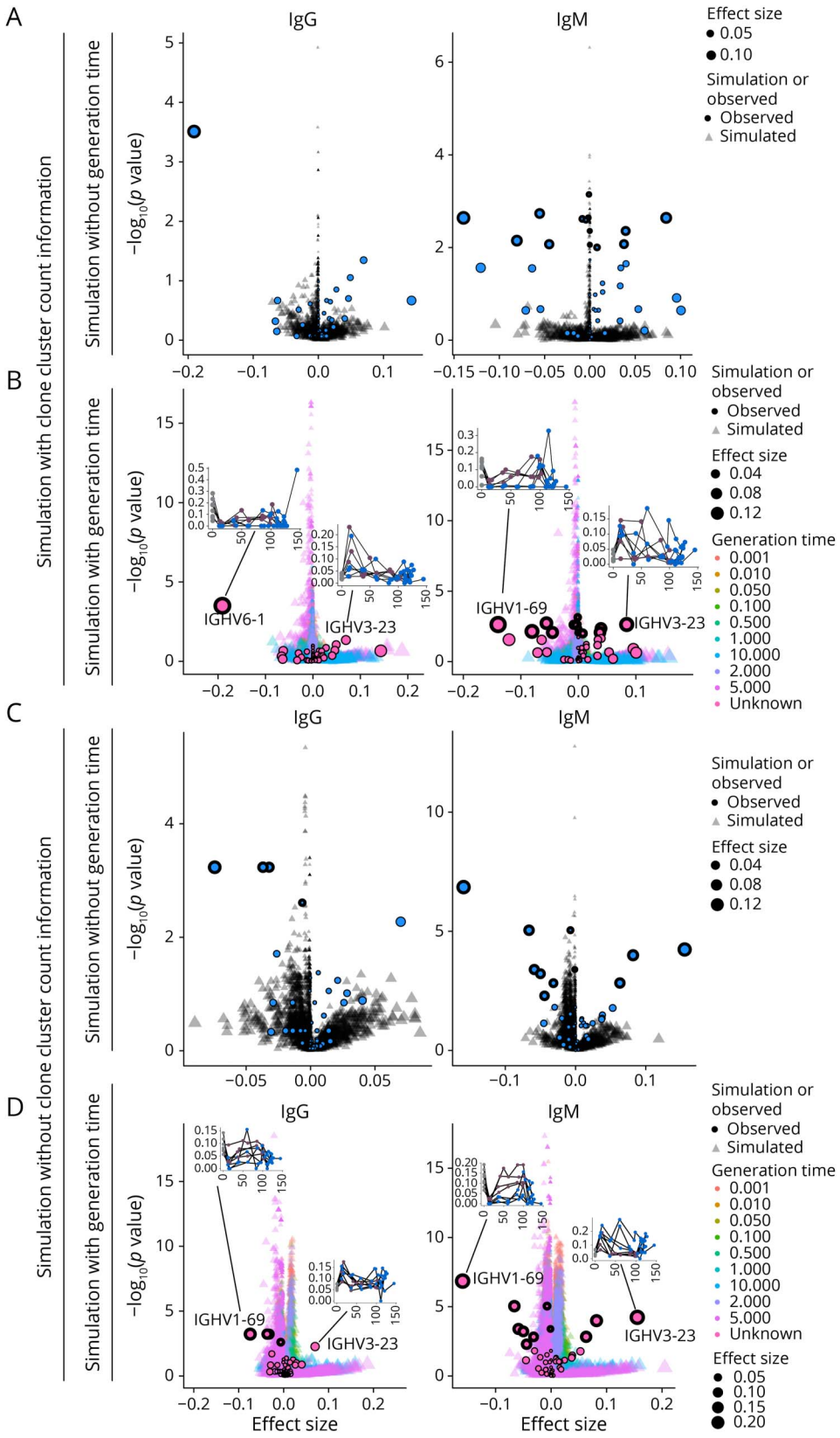

Each point represents the results of a single regression-based test on the effect of OCR on a given gene's prevalence. The x-axis gives the effect size of OCR on gene prevalence, and the y-axis gives the *p* value (*t* test) of the OCR covariate in the regression. The size of each point is proportional to the absolute value of the effect size. Transparent triangular points show the results of simulated data, and opaque circular points show the results of observed data. The color of each point signifies the generation time that was used for each simulated data point, with the exception of the observed values that have an unknown generation time. Observed data points with thick black borders had $p \leq 0.05$ (Benjamini-Hochberg corrected). The line graph insets show the observed data that the regression was performed on for hand-picked observed outlier genes: *IGHV1-69* and *IGHV3-23*. These show the V-gene prevalence time-series trajectories for each of the patients. The x-axis for these insets is weeks since baseline, the y-axis is V-gene prevalence, and each line is the trajectory for 1 patient. Blue-, purple-, and gray-colored points are OCR, IFNβ1-a, and untreated samples, respectively. (A and B) show results using V-gene prevalence values where counts of clone clusters are considered. (C and D) show results using V-gene prevalence values where only the presence/absence of clone clusters is considered (see Methods). (A, left and C, left) IgG data, without generation time in simulations. (A, right and C, right) IgM data, without generation time in simulations. (B, left and D, left) IgG data, with generation time in simulations. (B, right and D, right) IgM data, with generation time in simulations. IFN = interferon; Ig = immunoglobulin; OCR = ocrelizumab.

genes *IGHV1-69* and *IGHV3-23* were consistent outliers relative to the null simulations (Figure 5). Together, these results suggest that B cells harboring *IGHV3-23* are more likely to persist after OCR treatment, whereas those with *IGHV1-69* are more likely to be depleted.

Discussion

OCR is the first-approved CD20-targeting BCD therapy for RMS and PPMS. OCR-mediated BCD exhibits a rapid-onset clinical effect in the absence of substantial changes to serum Ig levels or CSF oligoclonal bands,[23-25] whereas long-term BCD has been associated with hypogammaglobulinemia.[26,27] B cells are professional APCs and support immune responses through cytokine production. Therefore, among this study's main objectives were to understand whether anti-CD20 therapy and deep peripheral BCD could alter the molecular TCR diversity of the circulating T-cell repertoire.

Herein, we demonstrated that the diversity of the circulating T-cell repertoire remains unaffected by OCR. Contrastingly, IFNβ1-a may alter the T-cell repertoire, in keeping with the known immunomodulatory response partially exerted by IFNβ1-a via effects on T-cell functions.[28] Potentially due to the small sample size, we did not observe a reduction of $CD8^+$ T cells as previously reported.[29] CD20-targeted therapies also deplete CD20-expressing T lymphocytes, a small subset of the overall T-cell compartment, some of which may target myelin antigens and may play a role in the pathogenesis of MS.[30,31] As we did not specifically explore effects on the TCR repertoire of $CD20^+$ T cells, we speculate that the depletion of this rare subpopulation in this small number of samples did not substantially affect the overall T-cell repertoire diversity.[32]

All B-cell subset levels dropped <0.1% of lymphocytes 12 weeks after OCR dosing, consistent with previous findings[33,34] and previously reported OCR treatment efficacy relationships.[35] In 3 patients, low levels of repopulating B cells were observed that included naive B cells, switched memory B cells, and plasmablasts. Because OCR does not deplete CD20-negative pro-B cells, it is possible that between OCR infusions, some pre-B cells matured to naive B cells, which then became detectable. Furthermore, given the very-low-level persistence of IgM- and IgG-expressing B cells in circulation over time, it is again possible that some of these B cells became detectable by flow cytometry as memory B cells and further mature plasmablasts, particularly toward the end of an OCR treatment cycle; they may have also originated from secondary lymphoid organs[36] following BAFF/APRIL pathway activation.[37] The overall deep BCD was accompanied by fewer unique BCRs per volume analyzed, corresponding to lowered levels of B-cell diversity. However, RepSeq revealed that some B-cell clonality and diversity persist longitudinally despite OCR treatment, suggesting the persistence of a functionally active B-cell repertoire potentially supporting adaptive immune functions. The presence of high-frequency clones under BCD suggests the persistence of clonally expanded B cells. A possible explanation could be the persistence of antigen-experienced B cells refractory to BCD due to their low CD20 expression.[22,38,39] We also found that IgM diversity is usually higher than IgG diversity at non–OCR-treated time points, but not at OCR-treated time points (eFigure 1, D and E, links.lww.com/NXI/A847), supporting the notion that persistent B cells are more likely to be antigen experienced (as naive B cells will be enriched in the IgM pool).

The observation of clonal relatedness between IgM- and IgG-expressing B cells during OCR therapy may imply active class-switch recombination and that functional antigen-driven B-cell activation and maturation are retained in the residual B-cell compartment. These results are consistent with recent vaccine studies in OCR-treated patients with MS, showing an attenuated, yet present, B-cell response to vaccination,[37] agreeing with our observations of a greatly diminished, yet persistent, BCR diversity, which retains a low-level ability for class switch recombination. Moreover, in line with our T-cell data, recent results show that although OCR-treated patients displayed a markedly reduced humoral response to SARS-CoV-2 vaccination,[40,41] they continued to generate SARS-CoV-2–specific T-cell responses comparable with healthy controls.[42]

Given the B-cell compartment's important role in the adaptive immune system, it is surprising that the deep BCD observed under OCR treatment is associated with a relatively favorable infectious disease safety profile. Indeed, despite not expressing the CD20 antigen, the plasma cell population is likely reduced over time due to depletion of its progenitor cells.[34] This suggests that repeated treatment cycles may lead to reduced plasma cell production and, as a result, hypogammaglobulinemia. None of the patients studied here developed hypogammaglobulinemia or associated serious infections during the observation period. It is therefore not possible to determine whether hypogammaglobulinemia is also associated with specific changes to the BCR. Nonetheless, this study's B-cell and T-cell repertoire results suggest a possible explanation for the relatively favorable infectious adverse event safety profile of OCR. Namely, the B-cell compartment appears to retain features necessary for normal adaptive immune function (e.g., class-switch recombination and repertoire diversity), and the T-cell repertoire diversity is largely maintained even after >3 years of BCD treatment. Future investigations could interrogate the BCR and TCR repertoires of patients treated with OCR and experiencing significant infections or hypogammaglobulinemia to see whether their diversity profiles differ from those reported here.

The role played by individual IGHV germline genes in autoimmune or anti-infectious B-cell responses has been extensively discussed. More recent evidence suggests that persistent clones post-BCD are enriched for autoantibodies in MG.[21,22] Thus, we sought to understand—in this small cohort of patients—if there are consistent biases determining which types of BCRs (i.e., V genes) remain in the repertoire after BCD. A decreased usage of *IGHV1-69* and an

overrepresentation of *IGHV3-23* after OCR treatment were observed. Previous work has shown that *IGHV1-69* is highly enriched in the naive/antigen inexperienced B-cell compartment, whereas *IGHV3-23* is generally more prevalent in the class-switched memory and plasmablast compartments.[8,43] This may suggest that antigen-experienced B cells are more likely to persist after OCR treatment.

Previous studies have shown that some pathogenic B cells may persist and that activated B cells may reemerge after BCD discontinuation,[33,44] which may suggest that BCD does not achieve full removal of the B-cell compartment. Indeed, our finding of longitudinally persistent clonally related B cells further substantiates the absence of a B-cell immune reset under OCR treatment. This suggests caution toward treatment cessation; however, larger studies are needed to test this.

Our analyses of samples collected for >3 years describe the behavior of, and possible interplay between, B- and T-cell repertoires in a therapeutically altered adaptive immune system. Nonetheless, several limitations are noted, including a small study population making it difficult to generalize findings to the MS population and the number of PBMCs collected per patient/time point representing a small sampling of the greater population, both with respect to tissue distribution and total lymphocyte populations present in an individual. Although we partially accounted for V gene amplification biases in our analysis, the absence of unique molecular identifiers limits this study. Although primer bias may artificially increase the prevalence of some V genes, potentially hindering the detection of changes in lower frequency V genes (thus affecting sensitivity), it is unlikely to cause false signals in our analyses because this effect would be consistent across all samples/time points. Trial randomization enabled the perfect segregation of patients by sexes across treatment arms. Although men have shown slightly lower TCR diversity than women in middle age,[45] this was not demonstrated in our patients' baseline (untreated) TCR diversity. Furthermore, because the OCR treatment arm comprised men, we would expect any OCR treatment-triggered decrease in TCR sequence diversity to be exacerbated by sex differences (rather than masked), whereas we see no difference. Future research in larger cohorts of OCR-treated patients should confirm these findings, explain their relevance for MS, and determine BCR and TCR repertoires in relation to clinical efficacy, hypogammaglobulinemia, and infectious adverse events. Nonetheless, our findings help to understand BCD's immunologic effects and adaptive immunity's resilience.

Acknowledgment

The authors thank the patients for their participation in this study. Editorial support (including assistance with revisions to the manuscript for nonintellectual content, figure redraws, and copyediting) was provided by Martha Hoque, PhD, of Articulate Science, United Kingdom, and funded by F. Hoffmann La-Roche.

Study Funding

This work was funded by F. Hoffmann La-Roche, the National MS Society (RG-4868), the NINDS (K02NS072288 and 5R01NS092835), and an endowment from the Westridge Foundation (to H.-C. von Büdingen and M.R. Wilson). S.A. Laurent was partially supported by the German Academic Exchange Service (DAAD). Editorial assistance was provided by Articulate Science, United Kingdom, funded by F. Hoffmann La-Roche.

Disclosure

S.A. Laurent reports no disclosures. During the conduct of this study, N.B.S. was a student at the University of California, San Francisco, and had no disclosures. After the completion of this study, N.B.S. became an employee of Genentech, Inc., and a shareholder of F. Hoffmann-La Roche Ltd. E.L. Eggers, H. Wu, B. Michel, and S. Demuth report no disclosures. A. Palanichamy is currently an employee of Spark Therapeutics, a subsidiary of F. Hoffmann-La Roche, Ltd. M.R. Wilson reports receiving grants from Roche/Genentech, during the conduct of the study. M. Sirota reports a financial relationship with TwoXAR for working as a Scientific Advisor outside the submitted work. R.D. Hernandez reports no disclosures. In the past 36 months, B.A.C. Cree has received personal compensation for consulting from Alexion, Atara, Autobahn, Avotres, Biogen, Boston Pharma, EMD Serono, Gossamer Bio, Hexal/Sandoz, Horizon, Immunic, Neuron23, Novartis, Sanofi, Siemens, TG Therapeutics, and Therini and received research support from Genentech. A.E. Herman is an employee of Genentech, Inc., and a shareholder of F. Hoffmann-La Roche Ltd. H.-C. von Büdingen reports receiving grants, personal fees, and nonfinancial reports from F. Hoffmann-La Roche Ltd during the conduct of this study; during the planning, initiation, and conduct of this study, he was employed by University of California, San Francisco, and received personal fees from F. Hoffmann-La Roche Ltd to participate in advisory boards. H.-C.v.B. is an employee and a shareholder of F. Hoffmann-La Roche Ltd. Go to Neurology.org/NN for full disclosure.

Publication History

Received by *Neurology: Neuroimmunology & Neuroinflammation* March 10, 2022. Accepted in final form February 22, 2023. Submitted and externally peer reviewed. The handling editor was Associate Editor Friedemann Paul, MD.

Appendix Authors

Name	Location	Contribution
Sarah A. Laurent, PhD	Department of Neurology, Weill Institute for Neurosciences, University of California, San Francisco, CA	Drafting/revision of the manuscript for content, including medical writing for content; major role in the acquisition of data; study concept or design; and analysis or interpretation of data
Nicolas B. Strauli, PhD	Biomedical Sciences Graduate Program, University of California, San Francisco, CA	Drafting/revision of the manuscript for content, including medical writing for content; study concept or design; and analysis or interpretation of data

Appendix *(continued)*

Name	Location	Contribution
Erica L. Eggers, BA	Department of Neurology, Weill Institute for Neurosciences, University of California, San Francisco, CA	Major role in the acquisition of data
Hao Wu, MD	Department of Neurology, Weill Institute for Neurosciences, University of California, San Francisco, CA	Analysis or interpretation of data
Brady Michel, PhD	Department of Neurology, Weill Institute for Neurosciences, University of California, San Francisco, CA	Major role in the acquisition of data
Stanislas Demuth, MD, MSc	Department of Neurology, Weill Institute for Neurosciences, University of California, San Francisco, CA	Major role in the acquisition of data
Arumugam Palanichamy, PhD	Department of Neurology, Weill Institute for Neurosciences, University of California, San Francisco, CA	Major role in the acquisition of data
Michael R. Wilson, MD	Department of Neurology, Weill Institute for Neurosciences, University of California, San Francisco, CA	Drafting/revision of the manuscript for content, including medical writing for content
Marina Sirota, PhD	Bakar Computational Health Sciences Institute and Department of Pediatrics, University of California, San Francisco, CA	Drafting/revision of the manuscript for content, including medical writing for content, and study concept or design
Ryan D. Hernandez, PhD	Department of Bioengineering and Therapeutic Sciences, University of California, San Francisco, CA; Department of Human Genetics, McGill University, Montreal, QC, Canada	Drafting/revision of the manuscript for content, including medical writing for content, and study concept or design
Bruce Anthony Campbell Cree, MD, PhD	Department of Neurology, Weill Institute for Neurosciences, University of California, San Francisco, CA	Drafting/revision of the manuscript for content, including medical writing for content
Ann E. Herman, PhD	OMNI Biomarker Development, Genentech, Inc., South San Francisco, CA	Drafting/revision of the manuscript for content, including medical writing for content
H.-Christian von Büdingen, MD	Department of Neurology, Weill Institute for Neurosciences, University of California, San Francisco, CA	Drafting/revision of the manuscript for content, including medical writing for content; study concept or design; and analysis or interpretation of data

References

1. Hauser SL, Bar-Or A, Comi G, et al. Ocrelizumab versus interferon beta-1a in relapsing multiple sclerosis. *N Engl J Med.* 2017;376(3):221-234. doi:10.1056/NEJMoa1601277
2. Montalban X, Hauser SL, Kappos L, et al. Ocrelizumab versus placebo in primary progressive multiple sclerosis. *N Engl J Med.* 2017;376(3):209-220. doi:10.1056/NEJMoa1606468
3. Li R, Patterson KR, Bar-Or A. Reassessing B cell contributions in multiple sclerosis. *Nat Immunol.* 2018;19(7):696-707. doi:10.1038/s41590-018-0135-x
4. Greenfield AL, Hauser SL. B-cell therapy for multiple sclerosis: entering an era. *Ann Neurol.* 2018;83(1):13-26. doi:10.1002/ana.25119
5. von Büdingen HC, Palanichamy A, Lehmann-Horn K, Michel BA, Zamvil SS. Update on the autoimmune pathology of multiple sclerosis: B-cells as disease-drivers and therapeutic targets. *Eur Neurol.* 2015;73(3-4):238-246. doi:10.1159/000377675
6. de Bourcy CFA, Dekker CL, Davis MM, Nicolls MR, Quake SR. Dynamics of the human antibody repertoire after B cell depletion in systemic sclerosis. *Sci Immunol.* 2017;2(15):eaan8289. doi:10.1126/sciimmunol.aan8289
7. Kowarik MC, Dzieciatkowska M, Wemlinger S, et al. The cerebrospinal fluid immunoglobulin transcriptome and proteome in neuromyelitis optica reveals central nervous system-specific B cell populations. *J Neuroinflammation.* 2015;12(1):19. doi:10.1186/s12974-015-0240-9
8. Glanville J, Kuo TC, von Büdingen H-C, et al. Naive antibody gene-segment frequencies are heritable and unaltered by chronic lymphocyte ablation. *Proc Natl Acad Sci U S A.* 2011;108(50):20066-20071. doi:10.1073/pnas.1107498108
9. von Büdingen H-C, Kuo TC, Sirota M, et al. B cell exchange across the blood-brain barrier in multiple sclerosis. *J Clin Invest.* 2012;122(12):4533-4543. doi:10.1172/JCI63842
10. Bolotin DA, Mamedov IZ, Britanova OV, et al. Next generation sequencing for TCR repertoire profiling: platform-specific features and correction algorithms. *Eur J Immunol.* 2012;42(11):3073-3083. doi:10.1002/eji.201242517
11. Eggers EL, Michel BA, Wu H, et al. Clonal relationships of CSF B cells in treatment-naive multiple sclerosis patients. *JCI Insight.* 2017;2(22):e92724. doi:10.1172/jci.insight.92724
12. Shannon CE. A mathematical theory of communication. *Bell Syst Tech J.* 1948;27(3):379-423.
13. Yager EJ, Ahmed M, Lanzer K, Randall TD, Woodland DL, Blackman MA. Age-associated decline in T cell repertoire diversity leads to holes in the repertoire and impaired immunity to influenza virus. *J Exp Med.* 2008;205(3):711-723. doi:10.1084/jem.20071140
14. Tabibian-Keissar H, Hazanov L, Schiby G, et al. Aging affects B-cell antigen receptor repertoire diversity in primary and secondary lymphoid tissues. *Eur J Immunol.* 2016;46(2):480-492. doi:10.1002/eji.201545586
15. Robins H. Immunosequencing: applications of immune repertoire deep sequencing. *Curr Opin Immunol.* 2013;25(5):646-652. doi:10.1016/j.coi.2013.09.017
16. Wright S. Evolution in Mendelian populations. *Genetics.* 1931;16(3):97-159.
17. Jewett EM, Steinrücken M, Song YS. The effects of population size histories on estimates of selection coefficients from time-series genetic data. *Mol Biol Evol.* 2016;33(11):3002-3027. doi:10.1093/molbev/msw173
18. Fedewa G, Radoshitzky SR, Chī X, et al. Ebola virus, but not Marburg virus, replicates efficiently and without required adaptation in snake cells. *Virus Evol.* 2018;4(2):vey034. doi:10.1093/ve/vey034
19. Strauli NB, Hernandez RD. Statistical inference of a convergent antibody repertoire response to influenza vaccine. *Genome Med.* 2016;8(1):60. doi:10.1186/s13073-016-0314-z
20. Qi Q, Liu Y, Cheng Y, et al. Diversity and clonal selection in the human T-cell repertoire. *Proc Natl Acad Sci U S A.* 2014;111(36):13139-13144. doi:10.1073/pnas.1409155111
21. Stathopoulos P, Kumar A, Nowak RJ, O'Connor KC. Autoantibody-producing plasmablasts after B cell depletion identified in muscle-specific kinase myasthenia gravis. *JCI Insight.* 2017;2(17):e94263. doi:10.1172/jci.insight.94263
22. Jiang R, Fichtner ML, Hoehn KB, et al. Single-cell repertoire tracing identifies rituximab-resistant B cells during myasthenia gravis relapses. *JCI Insight.* 2020;5(14):e136471. doi:10.1172/jci.insight.136471
23. Bar-Or A, Calabresi PAJ, Arnold D, et al. Rituximab in relapsing-remitting multiple sclerosis: a 72-week, open-label, phase I trial. *Ann Neurol.* 2008;63(3):395-400. doi:10.1002/ana.21363
24. Hauser SL, Waubant E, Arnold DL, et al. B-cell depletion with rituximab in relapsing–remitting multiple sclerosis. *N Engl J Med.* 2008;358(7):676-688. doi:10.1056/NEJMoa0706383
25. Piccio L, Naismith RT, Trinkaus K, et al. Changes in B- and T-lymphocyte and chemokine levels with rituximab treatment in multiple sclerosis. *Arch Neurol.* 2010;67(6):707-714. doi:10.1001/archneurol.2010.99
26. Perriguey M, Maarouf A, Stellmann J-P, et al. Hypogammaglobulinemia and infections in patients with multiple sclerosis treated with rituximab. *Neurol Neuroimmunol Neuroinflamm.* 2021;9(1):e1115. doi:10.1212/NXI.0000000000001115
27. Hauser SL, Kappos L, Arnold DL, et al. Five years of ocrelizumab in relapsing multiple sclerosis: OPERA studies open-label extension. *Neurology.* 2020;95(13):e1854-e1867. doi:10.1212/WNL.0000000000010376
28. Kasper LH, Reder AT. Immunomodulatory activity of interferon-beta. *Ann Clin Transl Neurol.* 2014;1(8):622-631. doi:10.1002/acn3.84
29. Abbadessa G, Maida E, Miele G, et al. Lymphopenia in multiple sclerosis patients treated with ocrelizumab is associated with an effect on CD8 T cells. *Mult Scler Relat Disord.* 2022;60:103740. doi:10.1016/j.msard.2022.103740
30. Sabatino JJ, Wilson MR, Calabresi PA, et al. Anti-CD20 therapy depletes activated myelin-specific $CD8^+$ T cells in multiple sclerosis. *Proc Natl Acad Sci U S A.* 2019;116(51):25800-25807. doi:10.1073/pnas.1915309116
31. Ochs J, Nissimov N, Torke S, et al. Proinflammatory $CD20^+$ T cells contribute to CNS-directed autoimmunity. *Sci Transl Med.* 2022;14(638):eabi4632. doi:10.1126/scitranslmed.abi4632
32. Palanichamy A, Jahn S, Nickles D, et al. Rituximab efficiently depletes increased CD20-expressing T cells in multiple sclerosis patients. *J Immunol.* 2014;193(2):580-586. doi:10.4049/jimmunol.1400118
33. Nissimov N, Hajiyeva Z, Torke S, et al. B cells reappear less mature and more activated after their anti-CD20–mediated depletion in multiple sclerosis. *Proc Natl Acad Sci U S A.* 2020;117(41):25690-25699.

34. Hauser S, Strauli N, Raievska A, et al. B-cell subset depletion following ocrelizumab treatment in patients with relapsing multiple sclerosis (4292). *Neurology*. 2021;96(15 Supplement):4292.
35. Gibiansky E, Petry C, Mercier F, et al. Ocrelizumab in relapsing and primary progressive multiple sclerosis: pharmacokinetic and pharmacodynamic analyses of OPERA I, OPERA II and ORATORIO. *Br J Clin Pharmacol*. 2021;87(6):2511-2520. doi:10.1111/bcp.14658
36. Dorcet G, Migné H, Biotti D, et al. Early B cells repopulation in multiple sclerosis patients treated with rituximab is not predictive of a risk of relapse or clinical progression. *J Neurol*. 2022;269(10):5443-5453. doi:10.1007/s00415-022-11197-6
37. Thai L-H, Le Gallou S, Robbins A, et al. BAFF and $CD4^+$ T cells are major survival factors for long-lived splenic plasma cells in a B-cell-depletion context. *Blood*. 2018;131(14):1545-1555. doi:10.1182/blood-2017-06-789578
38. Huang H, Benoist C, Mathis D. Rituximab specifically depletes short-lived autoreactive plasma cells in a mouse model of inflammatory arthritis. *Proc Natl Acad Sci U S A*. 2010;107(10):4658-4663. doi:10.1073/pnas.1001074107
39. Cho A, Bradley B, Kauffman R, et al. Robust memory responses against influenza vaccination in pemphigus patients previously treated with rituximab. *JCI Insight*. 2017;2(12):e93222. doi:10.1172/jci.insight.93222
40. Bar-Or A, Calkwood J, Chognot C, et al. Effect of ocrelizumab on vaccine responses in patients with multiple sclerosis: the VELOCE study. *Neurology*. 2020;95(14):e1999–e2008. doi:10.1212/WNL.0000000000010380
41. Khayat-Khoei M, Conway S, Rubinson DA, Jarolim P, Houtchens MK. Negative anti-SARS-CoV-2 S antibody response following Pfizer SARS-CoV-2 vaccination in a patient on ocrelizumab. *J Neurol*. 2021;268(10):3592-3594. doi:10.1007/s00415-021-10463-3
42. Brill L, Rechtman A, Zveik O, et al. Humoral and T-cell response to SARS-CoV-2 vaccination in patients with multiple sclerosis treated with ocrelizumab. *JAMA Neurol*. 2021;78(12):1510-1514. doi:10.1001/jamaneurol.2021.3599
43. Mroczek ES, Ippolito GC, Rogosch T, et al. Differences in the composition of the human antibody repertoire by B cell subsets in the blood. *Front Immunol*. 2014;5:96. doi:10.3389/fimmu.2014.00096
44. Häusler D, Häusser-Kinzel S, Feldmann L, et al. Functional characterization of reappearing B cells after anti-CD20 treatment of CNS autoimmune disease. *Proc Natl Acad Sci U S A*. 2018;115(39):9773-9778. doi:10.1073/pnas.1810470115
45. Britanova O, Shugay M, Merzllyak EM, et al. Dynamics of individual T cell repertoires: from cord blood to centenarians. *J Immunol*. 2016;196(12):5005-5013.